

THE INITIAL INSTABILITIES OF A GRANULAR BED UNDER A TURBULENT LIQUID FLOW

Erick de Moraes Franklin, franklin@fem.unicamp.br

Faculdade de Engenharia Mecânica - UNICAMP
Rua Mendeleev, 200, Cid. Universitária Zeferino Vaz
Campinas - SP

Abstract. *The transport of solid particles entrained by a fluid flow is frequently found in nature and in industrial environments. If shear stresses exerted by the fluid on the bed of particles are bounded to some limits, a mobile layer of particles takes place in which the particles stay in contact with the fixed bed, known as bed-load. The thickness of this mobile layer is a few particle diameters. Under these conditions, an initially flat bed of particles may be unstable, giving rise to ripples and dunes. These forms can be observed in nature, as for instance the sand dunes seen in deserts, but also in industrial applications, as, for example, the dunes appearing in petroleum pipelines conveying sand. In both cases, these forms grow until reaching a typical wavelength, this wavelength being highly correlated to their initial wavelength, which appears during the linear phase of the instabilities growth. So, the length scale of the initial linear instabilities is a key point to understand the typical structures observed in nature and in industrial facilities. We present here a theoretical and experimental study of the initial instabilities appearing in an initially flat bed of particles under a turbulent liquid flow, when bed-load is present. The theoretical work consists of a linear stability analysis of the problem. The experimental work consists in imposing different water flow rates over different beds of particles and in observing the appearance of initial instabilities (measuring their wavelength). From both the theoretical analysis and the experiments, we propose here, different from many previous studies, that the initial wavelengths of the instabilities vary with flow conditions when the fluid is a liquid.*

Keywords: *Instabilities, turbulent boundary-layer, bed-load*

1. INTRODUCTION

The transport of solid particles entrained by a fluid flow is frequently found in nature and in industrial environments. It is present, for example, in the erosion of bank rivers, in desert dunes displacement, in sand transport in hydrocarbon pipelines and in food industry granular transport. A better knowledge of this kind of transport is then of great importance to understand nature and also to improve particles related industrial procedures. Nevertheless, up to now, it has not been theoretically well understood.

When shear stresses exerted by the fluid flow on the bed of particles are able to move some of them, but are relatively small compared to particles weight, a mobile layer of particles known as bed-load takes place in which the particles stay in contact with the fixed bed. The thickness of this mobile layer is a few particle diameters.

Bed-load existence depends on the balance of two forces: a) an entraining force, of hydrodynamic nature, proportional to τd^2 , where τ is the bed shear stress and d is the mean particle diameter; b) a resisting force, in this case related to particles weight, proportional to $(\rho_s - \rho)gd^3$, where ρ is the density of the fluid, ρ_s is the density of the particles and g is the gravitational acceleration.

The relevant dimensionless parameter is the Shields number θ , which is the hydrodynamic force to weight ratio:

$$\theta = \frac{\tau}{(\rho_s - \rho)gd} \quad (1)$$

Bed-load takes place for $\theta = O(0.1)$.

Under the fluid flow, the flat bed may become unstable and deformed, generating ripples or dunes, which may grow and be displaced by the fluid flow. In a closed-conduit, such as hydrocarbon pipelines, those granular bed instabilities generate supplementary pressure loss. Moreover, as those forms migrate inside the conduit, they may generate pressure fluctuations. A better understanding of granular bed instabilities and its evolution is a key point to control sediment transport, as well as to understand nature.

We present here an experimental study concerning the initial instabilities of a granular bed by a turbulent liquid flow. The main goal of this work is to find the wavelength of these instabilities.

The next section describes the theory of initial instabilities of a granular bed sheared by a fluid flow. It is followed by a section containing an stability analysis applicable to our specific case, a section describing the experimental apparatus and a section presenting the main experimental results. Follows the conclusions section.

2. INITIAL INSTABILITIES OF A BED OF PARTICLES

Under the fluid flow, an initial flat granular bed may become unstable and deformed, generating ripples or dunes: there is an instability problem at the interface of two distinct phases. As one of these phases is not continuous, the problem becomes very complex, but with some assumptions the problem become treatable, giving us some clues about the behaviour of such instabilities.

The subject can be treated by an *hydrodynamics stability* approach if we suppose that the granular bed may have small perturbations compared to fluid flow scales. If this assumption is valid, the granular bed stability becomes a balance between local grains erosion and deposition. If there is erosion at the granular bed crests, the amplitude of initial perturbations of the bed decreases and the bed is stable. If there is deposition at the crests, the amplitude of initial perturbations of the bed grow and the bed is unstable. If there is neither erosion nor deposition at the crests, we have neutral stability.

The mass conservation of the grains in the granular bed link the height of the bed to the grains flux (see Eq. 11): it shows that there is erosion where the grains flux gradient is positive and deposition where the grains flux gradient is negative. So, the stability may be viewed as question of phase lag: if the maximum of the grains flow rate is upstream a crest, there is deposition at the crest and the bed is unstable. On the contrary, if the maximum of the grains flow rate is downstream a crest, there is erosion at the crest and the bed is stable. This is shown in Fig. 1. To answer the question of the instability conditions, we shall seek the mechanisms creating a phase lag between the shape of the granular bed and the grains flow rate. They are three: the fluid flow perturbation, the relaxation effects and the gravity.

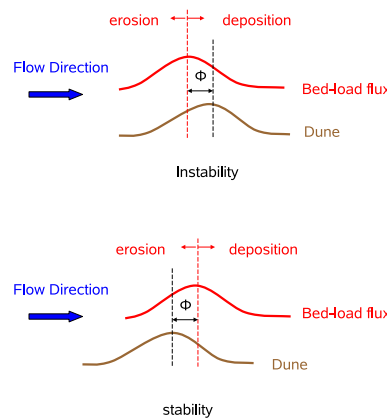


Figure 1. Sketch of the instability of a granular bed perturbation (called *dune* in the figure). ϕ is the shift of the maximum of the bed-load flux to the dune crest.

A ripple or a dune on a granular bed may be viewed as a perturbation of the surface that perturbs the fluid flow. The perturbation of the fluid flow by a hill with small aspect ratio, in the case of a turbulent boundary-layer, was analytically calculated by [Jackson and Hunt (1975)] and [Hunt et al. (1988)]. Those calculations were latter applied to the case of a barchan dune and other high aspect ratio forms by [Weng et al. (1991)]. [Jackson and Hunt (1975)], [Hunt et al. (1988)] and [Weng et al. (1991)] found that the perturbed shear stress is shifted upstream the dune crest. [Sauermaun (2001)] and [Kroy et al. (2002)] simplified the results of [Weng et al. (1991)] and obtained an expression containing only the dominant physical effects of this perturbation, making clear the reasons of this upstream shift. For a hill with a height h , a surface rugosity z_0 and a length $2L$ between the half-heights (so the total length is $\approx 4L$), they show that the longitudinal shear stress can be expressed in Fourier space as:

$$\hat{\tau}_k = Ah(|k| + iBk) \quad (2)$$

which in real space takes the form:

$$\hat{\tau}_x = A \left(\frac{1}{\pi} \int \frac{\partial_x h}{x - \xi} d\xi + B \partial_x h \right) \quad (3)$$

where k is a longitudinal wave-number, and A and B are considered as constants, as they vary as the logarithm of L/z_0 .

The Eqs. 2 and 3 show us, in a simple way, the form of the flow perturbation by a hill (or ripple or dune). The first term in the RHS of equation 3, the convolution product, is symmetric, similar to the potential solution of the flow perturbation by a hill. It comes from the pressure perturbations caused by the hill. The second term in the RHS of equation 3, which takes into account the local slope, is anti-symmetric. It comes from the non-linear inertial terms of the turbulent flow and can be seen as a second order correction of the potential solution, with minor changes in the magnitude of the first order solution, but causing an upstream shift. So, the perturbed fluid flow is the unstable mechanism.

On the other hand, when the shear stress conditions are changed, the bed-load flow rate will not instantaneously reach the corresponding equilibrium value. Instead, it will lag some distance (or some time) to reach equilibrium with the new stress conditions, which is related to an equilibrium (or saturation) length scale L_{sat} . L_{sat} is frequently associated to a drag length scale $l_{drag} = \frac{\rho_s}{\rho}d$ ([Elbelrhiti et al. (2005)] and [Claudin and Andreotti (2006)]). l_{drag} is an inertial length scale obtained when the density of the grain is many times bigger than the density of the fluid, $\rho_s \gg \rho$. It is then applied in situations when the fluid is a gas. When the fluid is a liquid, however, $\rho_s \approx \rho$ and it has been argued by [Charru (2006)], [Franklin (2008)] and [Franklin and Charru (2009)] that this length scale can no longer be applied. Instead, a relaxation length based on the deposition of a grain must be used $l_d = \frac{u_*}{U_s}d$.

In the case of a sinusoidal granular bed, the shear stress varies over it, so that the bed-load flow rate never is in equilibrium with the shear stress. Instead, the bed-load flow rate lags downstream to the shear stress perturbation, being then an stable mechanism.

A third mechanism affecting the stability of a sinuous granular bed is gravity and, because it tends to flat the surface, it is a stable mechanism. Even if gravity is not out-of-phase with regard to a sinuous bed, its effects generate a shift between the grains flow rate and the form of the bed: gravity difficults grains transport over positive slopes (upstream the bed crests) and facilitates grains transports over negative slopes (downstream the bed crests). So, if we consider initial granular bed perturbations (without boundary-layer separation), gravity causes a downstream shift of the maxima of grains flow rate, so that it is another stable mechanism.

From this point of view, the instability of a granular bed is a question of a shift of the maximum of the bed-load flow rate and the bed form: if the shift of the perturbed shear stress is larger than L_{sat} plus the gravity effects, the granular bed is unstable and ripples and dunes may appear. Otherwise, if the shift of the perturbed shear stress is lower than L_{sat} plus the gravity effects, the granular bed is stable and remains flat. This can be seen in a schematic way in Fig. 1.

Many works about granular bed instabilities under a fluid flow were made in the last decades. A great part of those works employed an hydrodynamic stability approach. A remarkable overview of this kind of work can be seen in [Engelund and Fredsoe (1982)].

[Coleman et al. (2003)] experimentally studied the granular bed instabilities under a closed-conduit turbulent flow, which is a case similar to our experiments (described latter in this paper). Their experiments were performed in a closed-conduit of rectangular cross section (6 m long, 0,1 m high and 0,3 m large), they used glass beads as granular matter ($\rho_p = 2680 \text{ kg/m}^3$) with mean diameters $d = 0,11 \text{ mm}$ and $d = 0,87 \text{ mm}$, and they used tap water as fluid. Water flow rate was varied so that they worked in between the following Reynolds numbers (based on the channel height): $40000 < Re < 110000$.

Based on their experiments, but also on some other previous experimental works, they found that the initial instabilities of a granular bed have a well defined wavelength, which scales with the grains diameters but not with the fluid flow. They propose the following expression for the initial wavelength:

$$\lambda = 175d^{0,75} \quad (4)$$

From Eq. 4, there is no correlation between λ and the fluid flow, which indicates that L_{sat} should be of inertial nature. Nevertheless, two critics may be made here:

- there is a great data dispersion present in [Coleman et al. (2003)]. This allows the utilisation of many experimental fittings, including some considering fluid flow effects;
- equation 4 has a dimensional inconsistency: λ is proportional to a diameter at a power 0,75 (so, the numerical constant have a dimension).

3. LINEAR STABILITY ANALYSIS

Even if a granular bed is not a continuous media, limiting the definition of small perturbations of the surface and the employment of a continuous spectra of normal modes, linear stability analysis have been carried out by many authors working on granular matter. Aware of this fact, we will proceed with a linear stability analysis of a granular bed sheared by a liquid flow.

We present here an analysis similar to the one presented by [Claudin and Andreotti (2006)] and [Elbelrhiti et al. (2005)]. The main difference here is the physical nature of the saturation length L_{sat} . Here, as shown below, we consider that this length scales with the deposition length $l_d = \frac{u_*}{U_s}d$, as proposed by [Charru (2006)]. To proceed with the analysis we need the equations describing the problem: the fluid flow perturbation by the granular bed undulations, the saturated flow rate of grains, the relaxation effects concerning the grains flow rate and the grains mass conservation. Gravity effects are not considered explicitly here (in fact, it can be considered implicitly in the saturated grains flow rate).

3.1 Fluid flow

The Fluid flow over a perturbed surface can be written as a base flow, unperturbed, plus a flow perturbation, if this perturbation is supposed small compared to the base flow. In terms of shear stress on the surface:

$$\tau = \tau_0(1 + \hat{\tau}) \quad (5)$$

where τ_0 is the base flow shear stress on the surface and $\hat{\tau}$ is a perturbation of the shear stress (here without dimension) due to a surface undulation. The perturbation of a turbulent boundary layer due to a small hill is given, in a simplified way, by Eq. 2 ([Kroy et al. (2002)] and [Sauermaann (2001)])

3.2 Saturated flow rate of grains

Under a steady state flow, and without spatial variations, the fluid flow and the grains flow rate are in equilibrium: the fluid flow entrains a certain amount of grains, which gets momentum from the fluid flow and dissipate it by impacts with the fixed part of the granular bed. So, the fluid flow capacity to transport grains is limited by this feed-back mechanism, and an equilibrium is reached if there is enough length (or time) to the development of this interaction. The grains flow rate in this equilibrium situation is known as saturated flow rate of grains q_{sat} . [Bagnold (1941)] has shown that:

$$q_{sat} \propto \tau^{3/2} \quad (6)$$

where q_{sat} is the saturated flow rate of grains. If the fluid flow rate is perturbed in a way like in Eq. 5:

$$\frac{q_{sat}}{Q_{sat}} = (1 + \hat{\tau})^{3/2} \quad (7)$$

where Q_{sat} is the flow rate of grains over a flat surface (base state). We can linearize this equation to find:

$$\frac{q_{sat}}{Q_{sat}} \sim 1 + \frac{3}{2}(Ah(|k| + iBk)) \quad (8)$$

3.3 Relaxation effects

In the case of a fluid flow over a perturbed granular bed (irregularities on the surface), the shear stress over the bed is always changing (Eq. 5). Concerning the grains flow rate, we expect that it will lag some distance (or time) with respect to the fluid flow. This distance is usually called *saturation length*, L_{sat} .

A simplified expression taking into account this relaxation effect can be obtained by the erosion-deposition model of [Charru (2006)] (Eq. 9). This equation, describing the relaxation of the grains flow rate due to fluid flow variations, is similar to the one obtained by [Andreotti et al. (2002)] (obtained by dimensional considerations).

$$\partial_x q = \frac{q_{sat} - q}{L_{sat}} \quad (9)$$

In [Andreotti et al. (2002)] and [Claudin and Andreotti (2006)], the saturation length is proportional to the travelling distance of individual grains, supposed of inertial origin $L_{sat} \sim l_{drag} = \frac{\rho_p}{\rho} d$. [Charru et al. (2004)] propose that, when the fluid is a liquid, the typical distance travelled by individual particles must be $l_d = \frac{u_*}{U_s} d$, which is related to the typical settling time of grains.

$$L_{sat} \sim l_d = \frac{u_*}{U_s} d \quad (10)$$

From Eq. 9, variations of the grains flow rate are always lagging with regard to the fluid flow, and this lag scales with L_{sat} .

3.4 Mass conservation

Exner equation gives the mass conservation of the fixed part of the granular bed (Eq. 11):

$$\partial_t h + \partial_x q = 0 \quad (11)$$

3.5 Normal modes and solution

Considering a granular bed with small perturbations, we can decompose the bed height h and the grains flow rate q in their normal modes:

$$h(x, t) = H e^{\sigma t - i\omega t + ikx} \quad (12)$$

$$\frac{q(x, t)}{Q_{sat}} = 1 + Q e^{\sigma t - i\omega t + ikx} \quad (13)$$

where k is the longitudinal wave-number, σ is the growth rate and ω is the pulsation. Inserting them into Eqs. 2, 8, 11 and 9, we find a 2 equations system:

$$(\sigma - i\omega)H + ikQQ_{sat} = 0 \quad (14)$$

$$(1 + ikL_c)Q = \frac{3}{2}(A|k| + iBk)H \quad (15)$$

which the non-trivial solution gives the growth rate σ and the pulsation ω of initial instabilities:

$$\sigma = \frac{3Q_{sat}k^2(B - A|k|L_{sat})}{2[1 + (kL_{sat})^2]} \quad (16)$$

$$\omega = \frac{3Q_{sat}k|k|(A + B|k|L_{sat})}{2[1 + (kL_{sat})^2]} \quad (17)$$

and the phase velocity of initial instabilities $c = \omega/k$ is:

$$c = \frac{3Q_{sat}|k|(A + B|k|L_{sat})}{2[1 + (kL_{sat})^2]} \quad (18)$$

3.6 Analysis

Most of linear stabilities studies of a granular bed give similar results, with variations of coefficients A and B and variations of the the saturation length L_{sat} . This length is zero in many analysis which do not take into account the relaxation effects of grains transport, and is of inertial origin in studies taking into account the relaxation effects. In our case, as we are dealing with liquids, L_{sat} is related to the typical time of grains settling (Eq. 10).

An example of numerical solution of Eqs. 16 and 18 can be seen in Fig. 2, where we did $A = B = 0, 1$, $L_{sat} = 1 \text{ mm}$ on the top of the figure and $L_{sat} = 10 \text{ mm}$ in the bottom of the figure. $U_s = 0, 01 \text{ m/s}$ is the typical settling speed of particles, $t_d = L_{sat}/U_s$ is the typical settling time of particles. We note that there is a cut-off wave-number: the small wave-numbers are always stable and the long unstable, which means a long-wave instability. Also, Eqs. 16 and 18 show us a preferential growth rate, allowing us to predict the most amplified wavelength.

Figure 2 also shows that the cut-off wave-number k_c , the most amplified wave-number k_A and the phase velocity c vary with L_{sat} almost in a linear way. As L_{sat} may be proportional to an inertial length (l_{drag}) or to a deposition length (l_d), values of k_c , k_A and c can be erroneous if the bad length is taken into account. We will try to prove here that the deposition length l_d is the scale to be considered in the case of liquids.

4. EXPERIMENTAL SET-UP

A closed-conduit experimental loop of rectangular cross-section (for simplicity, we name it “channel” in the following) and made of transparent material was used to investigate the dynamics of isolated dunes under a water flow.

Concerning the fluid flow, we are interested here in the fully turbulent regime. This can be defined in terms of the Reynolds number based on the cross section average velocity \bar{U} and on the conduit height H : $Re = \frac{\bar{U}H}{\nu} > 10000$, where ν is the kinematic viscosity. In the turbulent case, the shear velocity u_* is defined by $\tau = \rho u_*^2$.

In our experiments we employed water as the fluid media and some beads as granular media: glass beads with density $\rho_s = 2500 \text{ kg/m}^3$ and mean diameter $d = 0.5 \text{ mm}$, $d = 0.2 \text{ mm}$ and $d = 0.12 \text{ mm}$ and zirconium beads with density $\rho_s = 3800 \text{ kg/m}^3$ and mean diameter $d = 0.19 \text{ mm}$. Water flow rate varied between $6 \text{ m}^3/\text{h}$ and $10 \text{ m}^3/\text{h}$, what gives us the following range of Shields number θ and Reynolds number Re : $0.02 < \theta < 0.41$ and $13000 < Re < 24000$.

In order to have a good control of grains displacement and deformation under a permanent water flow, it is desirable to have low turbulence levels at the channel inlet. This was achieved by establishing a gravitational flow by means of a constant level head tank rather than the direct use of a pump.

The experimental loop is made of (figure 3):

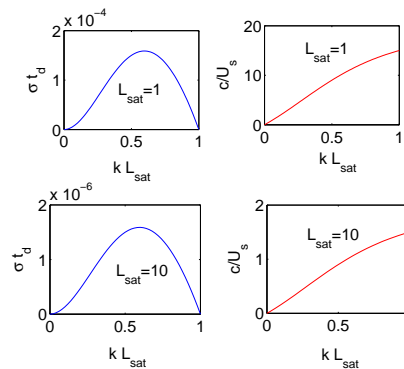


Figure 2. Example of non-dimensional growth rate σt_d and non-dimensional phase velocity c/U_s of initial perturbations.

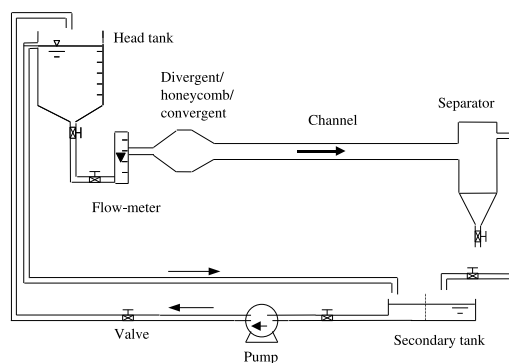


Figure 3. Experimental equipment.

- 1) A head tank. This constant water level tank gives a 2 m head pressure at the channel (test section). Water is continuously pumped to the tank (from the secondary tank) and the level is assured constant by an overflow passage (discharging in the secondary tank).
- 2) An electromagnetic flow-meter, which measures the fluid flow rate in the channel.
- 3) A divergent/honeycomb/convergent device, which can break large turbulent structures.
- 4) A channel (test section).
- 5) A fluid-particles separator. Particles settle due to a strong expansion (velocity reduction) of the fluid flow.
- 6) A secondary tank. The channel fluid flow and the head tank overflow are discharged in this tank. Water is continuously pumped from this tank to the head tank.
- 7) A water lifting pump, which continuously pumps water from the secondary tank to the head tank. The pumped water flow rate is larger than the water flow rate in the channel, maintaining the head tank water at a constant level.
- 8) Some valves to control the water flow rate.

The channel is a six meters long horizontal closed-conduit of rectangular cross-section (120 mm wide by 60 mm high), made of transparent material. One of the advantages of the rectangular cross-section channel is its plane horizontal surface. The fluid flow in this kind of channel is well-known ([Melling and Whitelaw (1976)]).

A mirror inclined at 45° made it possible the use of one single camera to obtain top and profile images of the granular bed instabilities. The camera, mounted on a rail system, was above the channel and had a direct top view of the dune. The mirror, close to one of the vertical sides, indirectly provided the granular bed profile image to the camera. An sketch of the camera/mirror device can be seen in Fig. 4.

The fluid flow upstream the bed of particles was measured with a PIV device. The PIV (Particle Image Velocimetry) measurements were made to find the fluid velocity profile $u(y)$ and the shear velocity u_{*w} on the vertical symmetry plane of the channel, for a mono-phase water flow. A description of the PIV device used can be seen in [Franklin (2008)] and [Franklin and Charru (2009)].

4.1 Experimental procedure

In order to decrease experimental uncertainty, we sieved the grains to obtain a distribution as tight as possible and prepared the initial granular bed always in the same manner. The employed grains are shown in Tab 1.

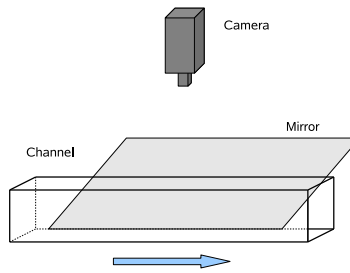


Figure 4. Image acquisition layout.

Matter	d_{min}	d_{max}	d_{moy}
...	μm	μm	μm
Glass	125	160	143
Glass	224	280	252
Glass	500	560	530
Zirconium	160	200	180

Table 1. Grains employed in experiments. d_{min} , d_{max} and d_{moy} correspond to inferior limits, superior limits and mean values, respectively

Concerning the initial granular bed (before the beginning of each experiment), we employed a special device to prepare it always with the same form and compactation. The initial granular beds were always 5 mm thick, 290 mm long and 100 mm large.

The experimental procedure was:

- with the channel previously filled with water, form the initial granular bed in a longitudinal position 4 m downstream the channel inlet;
- start, simultaneously, the water flow and the images recording;
- stop, simultaneously, the water flow and the images recording after the initial instabilities growth.

5. RESULTS

As soon as the water flow attained the desired flow rate, grains over the granular bed moved as bed-load and the granular bed become unstable: the initially flat bed was deformed giving rise to two-dimensional ripples, which evaluated to three-dimensional dunes. The transition to three-dimensional dunes was always with smaller velocities in the central part of the two-dimensional ripples than in the lateral parts (close to lateral walls). This can be seen in Fig. 5.

We are interested here in the initial instabilities, so we will deal here only with the two-dimensional ripples.

In order to determine the initial instabilities wavelength, we measured the distances between the crests of the initial two-dimensional ripples. The distance between crests was taken in the symmetry axis of the channel. Figure 6 presents the mean wavelength λ of initial ripples as a function of the grains diameter d . The mean values presented in Fig. 6 were computed for all grain types and water flow conditions. In this figure, symbols correspond to mean values of experimental results, error bars correspond to data dispersion and the line corresponds to Eq. 4, from [Coleman et al. (2003)]. The tendency of Eq. 4 seems to agree with experimental data, but the numerical coefficient present in Eq. 4 seems to superestimate the instabilities wavelength. We recall here that Eq. 4 has a dimensional inconsistency, so that its numerical constant has the dimensions of a length in power 0, 25.

Equation 4, which do not considers fluid flow conditions (it means a scaling with an inertial lengthscale), do not agrees well with our experimental data. In order to seek a better scaling to the initial instabilities of a granular bed sheared by a turbulent water flow, we remind here that its wavelength shall scale with the saturation length L_{sat} , and that L_{sat} should scale with the deposition length l_d , whenever the fluid is a liquid.

In order to verify if this assumption is correct, we present in the left part of Fig. 7 the initial wavelengths normalised by the grains diameter as a function of the water flow shear velocity u_{*w} (where the index w stands for *wall of the channel*). This figure shows an increasing of λ with the shear velocity (so, with the shear stress). This indicates that the liquid flow conditions shall be taken into account, so that the deposition length l_d seems to be the good length scale. Nevertheless we tried to verify this scaling by plotting λ/d as a function of u_{*w}/U_s , but it was not possible to find a tendency.

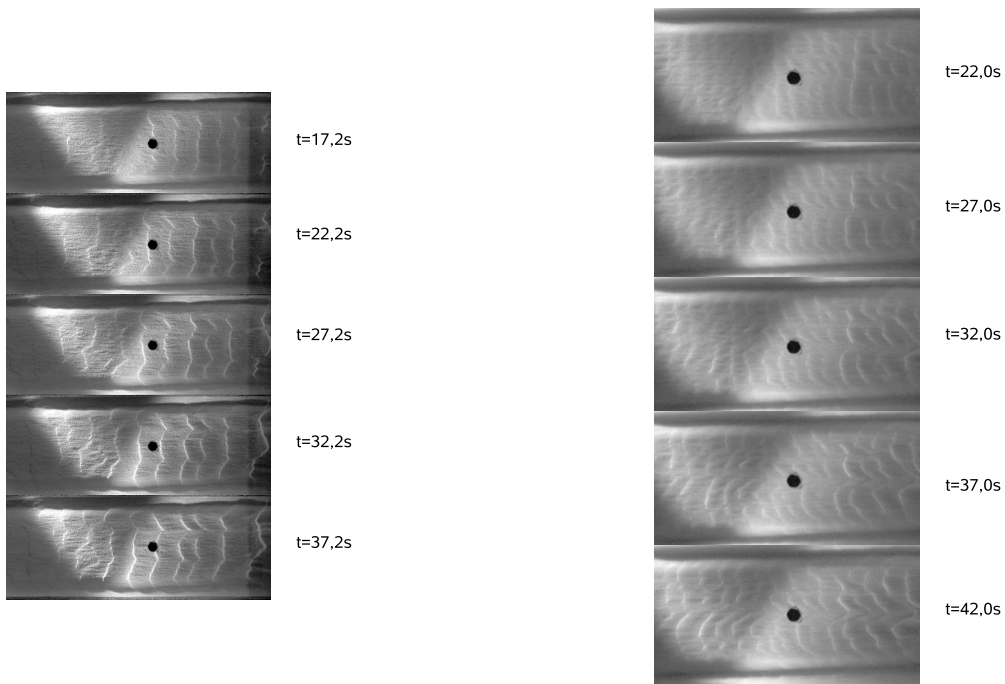


Figure 5. Initial wavelength of ripples λ of a granular bed sheared by a turbulent water flow and its evolution to three-dimensional forms. Flow direction is from right to left. In the left, $Re = 19900$ and the granular bed is composed of zirconium beads with $d_{moy} = 180 \mu m$. In the right, $Re = 14400$ and the granular bed is composed of glass beads with $d_{moy} = 143 \mu m$.

Another lengthscale present in this problem is the viscous length of the turbulent boundary-layer, ν/u_{*w} . Its pertinence in a fluid flow over a granular bed seems negligible, but two factors can justify it: (a) the two-dimensional ripples were always formed from the attack border of the initially flat bed, propagating downstream after; and (b) the viscous length in of the turbulent boundary-layer upstream the granular bed was of the same order of magnitude of the grains diameter: $\nu/u_{*w} \sim 0,1 mm$ and $d \sim 0,1 mm$. To verify if this lengthscale is present in the problem, we normalised the ripples wavelength and the grains diameter with the viscous length (note that the last becomes the particular Reynolds number). The right part of Figure 7 presents the non-dimension ripples wavelength λ^+ as a function of the particular Reynolds number Re_{*w} .

From Fig. 7, we can see that data is well aligned. Even if, at a first glance, the viscous length seems contradictory with the fluid flow over a granular bed, it seems to play a role in our case, were there is a transition from the channel wall to the granular bed. We note here that we have not varied the liquid viscosity, so one can question about the pertinence of the viscous length. Nevertheless, the shear velocity appears here as a characteristic scale of the problem.

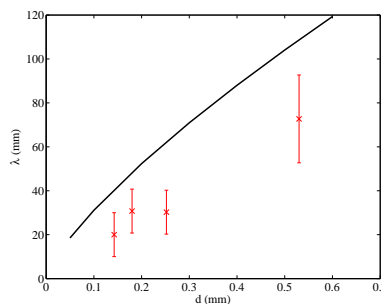


Figure 6. Initial wavelength of ripples λ of a granular bed as a function of grains diameter d (mean value for each type of grain and for all water flow conditions). Symbols and error bars correspond to experimental data. The line corresponds to Eq. 4.

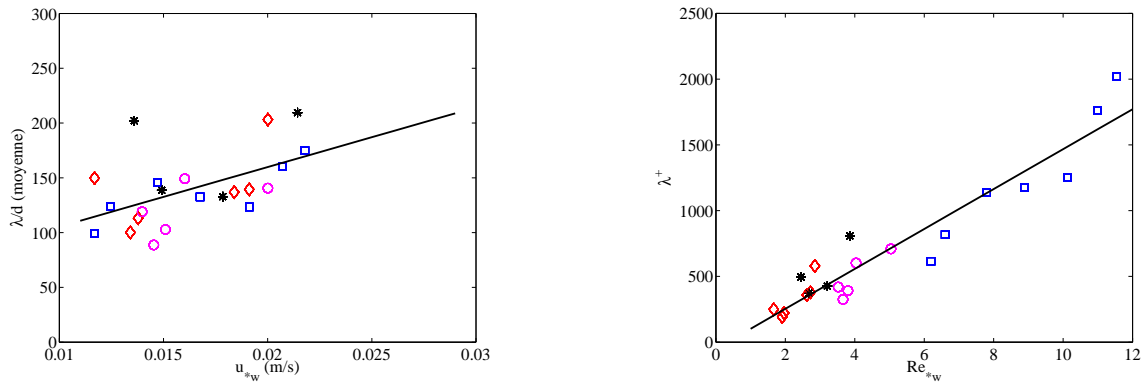


Figure 7. In the left, non-dimensional initial wavelength of ripples λ/d of a granular bed as a function u_{*w} . In the right, non-dimensional initial wavelength of ripples λ/d of a granular bed as a function Re_{*w} . The lozenge, circle, square and asterisk symbols correspond to $d = 0, 12 \text{ mm}$, $d = 0, 20 \text{ mm}$ and $d = 0, 50 \text{ mm}$ glass beads and to $d = 0, 19 \text{ mm}$ zirconium beads, respectively.

Considering that, in our case, the viscous length is a lengthscale, a fitting of the data present in Fig. 7 gives:

$$\lambda^+ = 152 (Re_{*w} - 0,33) \quad (19)$$

As we saw, Eq. 4 (from [Coleman et al. (2003)]) superestimates the initial wavelengths in our experiments. One of the reasons for that may come from its dimensional inconsistency, which may hide the influence of the fluid flow. In the proposed Eq. 19 there is no dimensional inconsistency and the fluid flow effects are taken into consideration. We can note that the data dispersion in Fig. 6 (error bars) tends to be aligned when the water flow is taken into account (Fig. 7)

In summary, we could not prove a direct link between the wavelengths of the initial instability of a granular bed and the deposition lengthscale $l_d = \frac{u_{*w}}{U_s} d$. Nevertheless, different from previous works, we propose that the initial wavelengths varies with fluid flow conditions whenever the fluid is a liquid. This refutes the utilisation of an inertial length in the scaling of the initial instabilities of a granular bed under a turbulent liquid flow.

6. CONCLUSION

The transport of solid particles as bed-load may, in some cases, make an initially flat granular bed give rise to ripples or dunes, which may grow and be displaced by the fluid flow. In a closed-conduit, such as hydrocarbon pipelines, those granular bed instabilities generate supplementary pressure loss. Moreover, as those forms migrate inside the conduit, they may generate pressure fluctuations. A better understanding of granular bed instabilities and its evolution is a key point to control sediment transport, as well as to understand nature.

We have investigated theoretically and experimentally the instabilities of a granular bed sheared by a turbulent liquid flow. The theoretical work consisted of a linear stability analysis of the granular bed and the experimental work consisted of instability experiments of a flat granular bed in a turbulent closed-conduit flow.

The stability analysis showed that the saturation lengthscale L_{sat} is an important scale of the problem. Also, as the dimensional analysis indicate that, when the fluid is a liquid, the saturation length must be proportional to the deposition length, our analysis show that $\lambda \sim L_{sat} \sim l_d = \frac{u_{*w}}{U_s} d$. So, different from previous stability analysis, we show here that the initial wavelengths vary with the liquid flow conditions.

Acquired data shown in this paper concerns image recording of the granular bed evolution in time and PIV measurements of pure water flow in a closed-conduit ([Franklin (2008)]). From experimental data, we can see that the initial instabilities are two-dimensional ripples, and that they vary with the liquid flow conditions.

We could not prove a direct link between the wavelengths of the initial instability of a granular bed and the deposition lengthscale $l_d = \frac{u_{*w}}{U_s} d$. Nevertheless, different from previous works, we propose that the initial wavelengths varies with fluid flow conditions whenever the fluid is a liquid. This refutes the utilisation of an inertial length in the scaling of the initial instabilities of a granular bed under a turbulent liquid flow.

In cases where there is a transition from a smooth wall to a granular bed, and whenever the fluid shearing the bed is a liquid, we propose an original relation to the initial instabilities wavelengths.

7. ACKNOWLEDGEMENTS

The author is grateful to Prof. François Charru, who was his PhD. thesis advisor (this work is a part of the author PhD. thesis) and to the Institut de Mécanique des Fluides de Toulouse, where all this work was done.

8. REFERENCES

- Andreotti, B., Claudin, P. and Douady, S., 2002, "Selection of dune shapes and velocities. Part2: a two-dimensional model", *Eur. Phys. J. B*, Vol.28, pp. 341-352.
- Bagnold, R.A., 1941, "The physics of blown sand and desert dunes", Ed. Chapman and Hall, London, England.
- Charru, F., Mouilleron-Arnould, H. and Eiff, O., 2004, "Erosion and deposition of particles on a bed sheared by a viscous flow", *Journal of Fluid Mechanics*, Vol.519, pp. 55-80.
- Charru, F., 2006, "Selection of the ripple length on a granular bed sheared by a liquid flow", *Physics of Fluids*, Vol.18, 121508.
- Claudin, P. and Andreotti B., 2006, "A scaling law for aeolian dunes on Mars, Venus, Earth, and for subaqueous ripples", *Earth and Planetary Science Letters*, Vol.252, pp. 30-44.
- Coleman, S.E., Fedele, J.J. and Garcia M.H., 2003, "Closed-conduit bed-form initiation and development", *J. Hydraul. Eng.*, Vol.129, pp. 956-965.
- Elbelrhiti, H., Claudin, P. and Andreotti B., 2005, "Field evidence for surface-wave-induced instability of sand dunes", *Nature*, Vol.437, 04058.
- Engelund, F. and Fredsoe, J., 1982, "Sediment ripples and dunes", *Ann. Rev. Fluid Mech.*, Vol.14, pp. 13-37.
- Franklin, E.M., 2008, "Dynamique de dunes isolées dans un écoulement cisailé", PhD. Thesis, Université de Toulouse III.
- Franklin, E.M. and Charru, F., 2007, "Dune Migration in a Closed-conduit Flow", *Proceedings of the International Conference in Multiphase Flow*, Leipzig, Germany.
- Franklin, E.M. and Charru, F., 2009, "Morphology and displacement of dunes in a closed-conduit flow", *Powder Technology*, Vol.190, pp. 247-251.
- Hunt, J.C.R., Leibovich, S. and Richards, K.J., 1988, "Turbulent shear flows over low hills", *Quarterly Journal of the Royal Meteorological Society*, Vol.114, pp. 1435-1470.
- Jackson, P.S. and Hunt, J.C.R., 1975, "Turbulent wind flow over a low hill", *Quarterly Journal of the Royal Meteorological Society*, Vol.101, pp. 929-955.
- Kroy, K., Sauermann, G. and Herrmann, H.J., 2002, "Minimal model for aeolian sand dunes", *Physical Review E*, Vol.66, 031302.
- Melling, A. and Whitelaw, J.H., 1976, "Turbulent flow in a rectangular duct", *Journal of Fluid Mechanics*, Vol.778, pp. 289-315.
- Sauermann, G., 2001, "Modeling of wind blown sand and desert dunes", PhD Thesis.
- Weng, W.S., Hunt, J.C.R., Carruthers, D.J., Warren, A., Wiggs, G.F.S., Livingstone, I. and Castro, I., 1991, "Air flow and sand transport over sand-dunes", *Acta Mechanica*, Suppl 2, 1, pp. 1-22.

9. Responsibility notice

The author(s) is (are) the only responsible for the printed material included in this paper